



Monte Carlo simulation of the EBIC grain boundary contrast in semiconductors

N. Tabet^{a,*}, M. Ledra^b

^aKing Fahd University of Petroleum and Minerals, Physics Department, P.O. Box 477, Dhahran 31261, Saudi Arabia

^bUniversity of Biskra, Physics Department, Biskra, Algeria

Abstract

The electron beam induced current (EBIC) recombination contrast of grain boundaries (GB) is calculated by means of a Monte Carlo simulation algorithm. After considering a pointlike generation source, a three-dimensional distribution of pointlike sources is simulated and used to calculate the EBIC profiles across the grain boundary. In both cases, we observe a saturation of the maximum EBIC contrast as the carrier lifetime within the GB decreases. The results show, for a three dimensional electron probe, a linear dependence of the contrast on the GB width. In addition, extrapolated values of the maximum contrast obtained for a zero width GB are in good agreement with that calculated by analytical models.

Keywords: Electron beam induced current; Grain boundaries; Semiconductors

1. Introduction

The electron beam induced current (EBIC) technique is a powerful method which has been extensively used to image the recombination activity of extended defects in semi-conductors. Many theoretical models which are based on the solution of the continuity equation, have been developed to analyze the collected current near dislocations and grain boundaries, [1–3]. These models often lead to complicated mathematical expressions of the collected current unless the defect has some symmetry or/and simplifications are made. When analytical models become intractable, numerical simulations offer a practical alternative.

The EBIC contrast of a grain boundary is known, from experimental results as well as from theoretical works, to depend on both the GB recombination efficiency and the bulk properties of the semiconductor [4–6]. Theoretical models describe this dependence through the recombination velocity v_s and the bulk diffusion length. The recombination velocity is defined by means of the ratio

$$v_s = \frac{J_{gb}}{\Delta p} \quad (1)$$

* Corresponding author. Fax: +966 3 8602293; e-mail: tabet@ccse.kfupm.edu.sa

where, J_{gb} is the component of the carrier flux normal to the GB plane, and where Δp is the density of the excess minority carriers at the GB plane. These models describe the GB as a two dimensional defect. However, many experimental observations show that the electrical activity of GB is related to the presence of segregated impurities in the vicinity of the GB. As a result, it is needed to consider the GB as a region whose extension ω_{gb} depends on the sample under investigation.

In this paper, we present the results of a Monte Carlo simulation of the EBIC contrast based on the above description of the GB. The effects of the GB width and of the carrier lifetime within the GB region are analyzed. We consider first the simple case of a single pointlike source generation. Then, the results are compared with those obtained by using a 3-dimensional generation.

2. Pointlike source generation

Under an electron beam excitation, the carriers are generated within a volume whose size depends on the beam energy. The collected current can be considered as the result of the contributions of pointlike sources distributed within the generation volume. Therefore, it

is of interest to calculate the EBIC contrast which corresponds to an ideal zero-size electron probe. Computations have been made following the algorithm described in Ref. [7]. The carrier lifetimes within the bulk, τ_b , and within the GB region, τ_{gb} , are assumed to be constant. The random motion of the carriers is simulated by considering successive time steps, Δt , which corresponds to a small fraction of the carrier lifetime at the considered point of the sample. The distance crossed by carrier during Δt is given by

$$\Delta R = (D\Delta t)^{1/2} \quad (2)$$

where D is the effective diffusion coefficient. The diffusion coefficient is related to the carrier mobility and thus, depends on the doping level and the material under consideration. Furthermore, two different values D_b and D_{gb} should be considered for the bulk and the GB regions, respectively. Nevertheless, we have used in our calculations a constant value for D which is equal to $1 \text{ cm}^2 \text{ s}^{-1}$. The available theoretical models use also the same diffusion coefficient within the defect and the bulk. Different values of D_b and D_{gb} can be introduced in the simulations when experimental data are analyzed. The average collection probability has been obtained by simulating the motion of up to 2×10^3 carriers.

Fig. 1 displays typical EBIC profile across a GB. It is common to define the maximum contrast as follows

$$C_{\max} = \frac{(I - I_0)}{I_0} \quad (3)$$

where I_0 and I are the collected currents when the incident electron beam is far away from the GB and

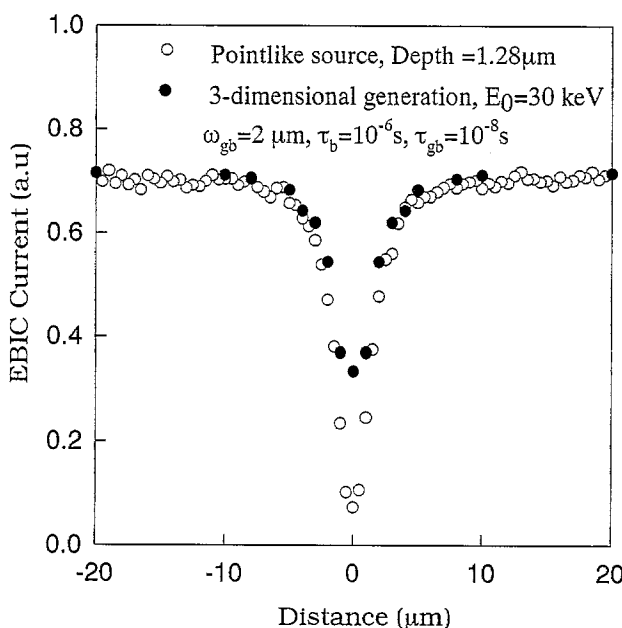


Fig. 1. EBIC contrast profiles across a $2 \mu\text{m}$ width grain boundary.

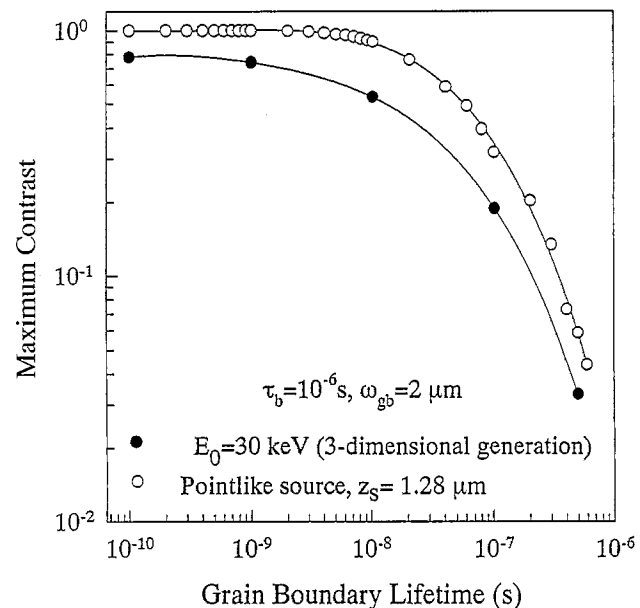


Fig. 2. Variation of the EBIC contrast vs. the carrier lifetime within the grain boundary.

within the GB, respectively. The contrast C_{\max} depends on the recombination velocity and the bulk lifetime [6]. In the present approach, we have considered separately the maximum contrast dependencies on the GB width ω_{gb} and on the lifetime τ_{gb} . Fig. 2 displays the C_{\max} dependence on the GB lifetime. It appears clearly that C_{\max} is not a linear function of the recombination velocity defined by the ratio $(0.5 \omega_{gb}/\tau_{gb})$. In the case of the GB which is considered in Fig. 2, the EBIC contrast has been found proportional to $(\tau_{gb})^{-0.7}$ in the low contrast region. As the GB lifetime decreases, a saturation of the contrast occurs.

Fig. 3 displays the variation of the maximum contrast versus the GB width. The saturation of the contrast which occurs for wide GB can be explained as follows. When the GB width becomes larger than the carrier diffusion length L_{gb} ($= \sqrt{D_{gb}\tau_{gb}}$), the collected current I is mainly determined by the source depth z_s and the diffusion length L_{gb} while I_0 is determined by z_s and the bulk length L_b ($= \sqrt{D_b\tau_b}$).

3. Three dimensional generation

A three dimensional distribution of pointlike sources is calculated by means of a Monte Carlo simulation of the trajectories of the primary electrons. The computations have been carried out for a germanium sample. It can be pointed out that the same distribution of the point sources can be used for GaAs whose mean atomic number is equal to that of germanium ($Z = 32$). Fig. 4 displays the electron trajectories for a 30 keV beam. The beam size was taken equal to zero. In order to

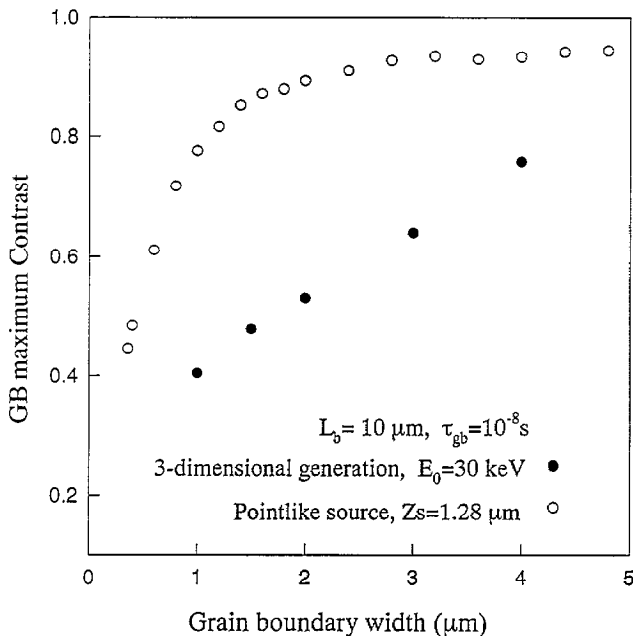


Fig. 3. Variation of the maximum EBIC contrast vs. the grain boundary width.

study the effect of the spatial expansion of the generation function on the contrast, we have considered a pointlike source depth which gives the same collected current as the 3-dimensional electron probe far away from the grain boundary. This value has been found equal to $1.28 \mu\text{m}$ for $E_0 = 30$ keV. It corresponds approximately to $R/3$, R being the electron range in

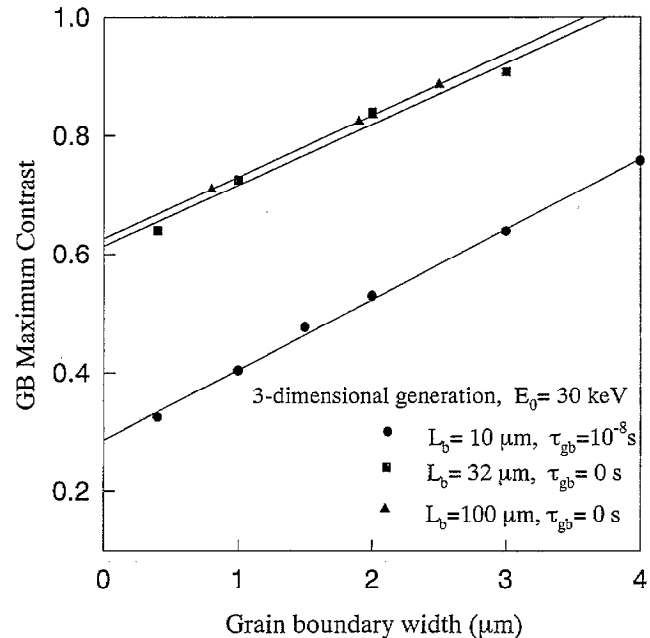


Fig. 5. Variation of the maximum EBIC contrast for different values of the bulk diffusion length and GB lifetime.

germanium for a 30 keV beam [8].

In Fig. 1 the contrast profiles across a GB for a pointlike and 3-dimensional generation are compared. The maximum contrast is sensitively lowered by the spatial expansion of the electron probe. Fig. 2 shows that the contrast dependence on the GB lifetime is slightly affected. A saturation of the maximum contrast

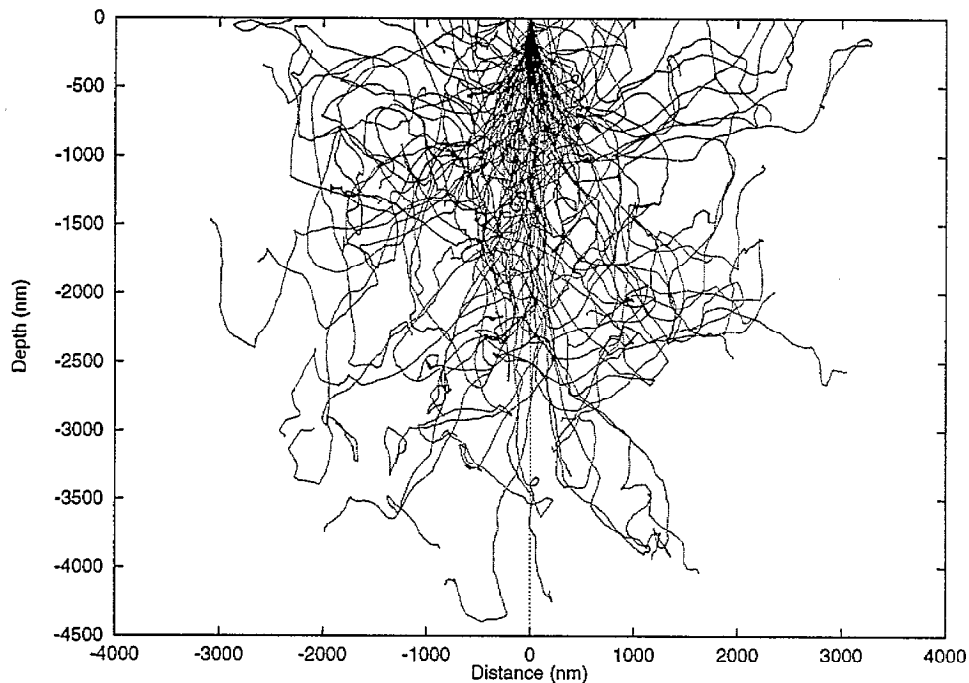


Fig. 4. Electron trajectories in Ge for a 30 keV beam. The beam size is taken equal to zero.

is noticed as the carrier lifetime within the GB decreases. As for Fig. 3, it shows a drastic effect of the electron probe size on the variation of the contrast with the GB width. A quasi linear dependence of the maximum contrast on the GB width is obtained for a 3-dimensional generation while for a pointlike probe, the contrast increases rapidly with the GB width then saturates.

We have carried out calculations for a GB with $\tau_{gb} = 0$, i.e. the recombination probability of each minority carrier which reaches the GB region is taken equal to 1. The results are displayed in Fig. 5. The variation of the maximum contrast, for a 30 keV beam energy, can be described by the following expression

$$C_{\max} = C_{\max}(0) + 0.1 \times \omega_{gb} \quad (4)$$

where ω_{gb} is expressed in micrometers and where $C_{\max}(0)$ corresponds to the maximum contrast of a zero width grain boundary. Donolato showed by using an analytical model that $C_{\max}(0)$ increases as the bulk diffusion length and the GB recombination velocity increase. $C_{\max}(0)$ saturates at a value which lies between 0.64 and 0.67 [9]. Our results displayed in Fig. 4 lead to an upper limit of $C_{\max}(0)$ equal to 0.62.

4. Conclusion

Monte Carlo simulation of the EBIC contrast has been carried out by considering both a pointlike source and a 3-dimensional generation. The results show that

the dependence of the maximum contrast on the GB width is very sensitive to the electron probe size. An upper limit of the zero width GB maximum contrast equal to 0.62 has been obtained. This value is in good agreement with that calculated by using an analytical model. The effect of the GB width has been separated from that of the carrier lifetime within the GB region. Such approach is appropriate to analyze the EBIC contrast of real GB whose width cannot be neglected, in most cases, due to the impurity segregation.

Acknowledgements

Tabet would like to thank King Fahd University of Petroleum and Minerals for his support.

References

- [1] L. Pasemann, in J.H. Werner and H.P. Strunk (eds.), *Polycrystalline Semiconductors II*, Springer, Berlin, 1991, p. 62.
- [2] Y. Marfaing and J.L. Maurice, *J. Phys. IV, Coll. C6, Suppl. J. Phys. III*, 1 (1991) 77.
- [3] B. Sieber, *Philos. Mag.*, B55 (5) (1987) 585.
- [4] N. Tabet, in J.L. Walter, A.H. King and K. Tangri (eds.), *Structure and Property Relationships for Interfaces*, 1991, p. 361.
- [5] J. Marek, *J. Appl. Phys.*, 55 (1984) 318.
- [6] C. Donolato, *J. Appl. Phys.*, 54 (1983) 131.
- [7] M. Stemmer, *Mater. Sci. Eng.*, B24 (1994) 180.
- [8] C.J. Wu and D.B. Wittry, *J. Appl. Phys.*, 49 (1978) 2827.
- [9] C. Donolato, *Mater. Sci. Eng.*, B24 (1994) 61.